Light Quark Resonances in $\bar{p}p$ Annihilations at 5.2 GeV/c

I. Uman, D. Joffe*, Z. Metreveli, K. K. Seth, A. Tomaradze, and P. Zweber

Northwestern University, Evanston, Illinois 60208

Data from the Fermilab E835 experiment have been used to study the reaction $\bar{p}p \to \eta\eta\pi^0$ at 5.2 GeV/c. A sample of 22 million six photons events has been analyzed to construct the Dalitz plot containing $\sim 80k$ $\eta\eta\pi^0$ events. A partial wave analysis of the data has been done. Six f_J-states decaying into $\eta\eta$ and five a_J-states decaying into $\eta\pi^0$ are identified in the mass region ~ 1.3 and 2.4 GeV, and their masses, widths and spins are determined by maximum likelihood analysis of the data. Two f_0 states are identified with the popular candidates for the lightest scalar glueball, $f_0(1500)$ and $f_0(1710)$.

I. INTRODUCTION

Antiproton-proton annihilations leading to final states containing light-quark structures constitute very attractive and powerful tools for the study of the spectroscopy of $q\bar{q}$ mesons, glueballs, and hybrids. Indeed, major contributions to light-quark spectroscopy have been made by the study of $\bar{p}p$ interactions with stopped and low energy antiprotons [1]. In this paper we report a study of the isoscalar and isovector light quark resonances populated in the reaction $\bar{p}p \to \eta\eta\pi^0$ in the collision of 5.2 GeV/c antiprotons with protons at rest. The reaction is very selective. It can only populate $q\bar{q}$ states with $J^{PC} = even^{++}$, isoscalar, or f-states decaying into $\eta\eta$, and isovector, or a-states decaying into $\eta\pi^0$. The $\eta\eta$ states may contain admixtures of low lying 0^{++} and 2^{++} glueballs, and the $\eta\pi^0$ states may include states with non-$q\bar{q}$ J^{PC}, such as the 1^{-+} hybrids.

In the spectroscopy of light-quark mesons there remain many open questions. Theoretical calculations [2] for states with angular momentum $L \leq 4$ predict twelve f_J-states, and six a_J-states in the mass range 1 GeV-2.5 GeV. In addition, two glueball states, with $I = 0$, $J^{PC} = 0^{++}, 2^{++}$, and at least one manifestly exotic $q\bar{q}g$ hybrid with $I = 1$, $J^{PC} = 1^{-+}$ are predicted in this mass range. In different experiments many f_0 and f_2 states have been claimed, but PDG'04 [3] considers only four f_0 states, four f_2 states, and five $a_{0,2,4}$ to be established well enough to be included in the meson summary list. In the present investigation we present new determinations of masses and J^{PC} of several of the established f_J and a_J states, and provide evidence for several previously unconfirmed states.

II. DATA AND EVENT SELECTION

In the present analysis data from Fermilab $\bar{p}p$ annihilation experiment E835 is used. The stored and cooled antiprotons circulating in the Fermilab Antiproton Accumulator intersect a hydrogen cluster jet gas target, and the reaction products are detected in a detector system which surrounds the interaction region. Full details of the detector and its performance can be found elsewhere [4]. Photons are detected in the lead glass central detector in the angular range $10.6^o < \theta < 70.0^o$ and 2π in ϕ, with an energy resolution of $\frac{\sigma_E(E)}{E} = \frac{0.06}{\sqrt{E(GeV)}} + 0.04$. Luminosity was measured by detecting recoil protons at $\sim 87.5^o$. The data were collected at $\bar{p}$ momenta of 5.2 GeV/c corresponding to center of mass energy range of $E_{cms} = 3.409 - 3.418$ GeV with a total luminosity of $11.4pb^{-1}$.

The reaction studied was

$$\bar{p}p \to \pi^0\eta\eta, \quad \pi^0 \to 2\gamma, \quad \eta \to 2\gamma$$

Twenty two million six photon events were recorded in the full detector, of which 3.25 million were fully contained in the fiducial volume, had no photons in the forward calorimeter, and met the energy-momentum (4C) constraint with probability $> 10\%$. Of these, 139,500 events passed $\eta\eta\pi^0$ seven constraint fit with $CL > 10\%$. These events were then subjected to three 'anticuts'. Events which met the hypotheses for the 'contaminant' final states $(\pi^0\pi^0\pi^0)$, $(\eta\pi^0\pi^0)$ or $(\eta\eta\eta)$ with $CL > 2\%$ were removed, and the final sample of 83,400 events was used for the Dalitz plot analysis. The Dalitz plot and its $\eta\eta$ and $\eta\pi^0$ projections are shown in Fig. 1. These mass distributions differ completely from the phase space distributions which are predicted to be essentially flat over the entire $1.0 - 2.6$ GeV/c^2 mass region for both $M(\eta\eta)$ and $M(\eta\pi^0)$. Visible structures appear to correspond in the $\eta\eta$ diagonal to $f_0(1500)$, $f_0(1710)$, and a complex of states in the mass region of $\simeq 2000 - 2250$ MeV. The visible horizontal and vertical $\eta\pi^0$ bands appear to correspond to $a_0(980)$ and a state around 1300 MeV. It is important to keep in mind that the 'anticuts' described above remove events and introduce distortions in specific regions of the Dalitz plot. The effect of the $3\pi^0$ 'anticut' was large, but mostly confined to the diagonal edge of the Dalitz plot in the $f_2(1270)$ region. The effect of the $\pi^0\pi^0\eta$ 'anticut' was smaller and also largely confined to the $f_2(1270)$ and $f_0(1370)$ regions. The effect of 3η

'anticut' was small, and was mainly in the vicinity of $a_2(1320)$.

Monte Carlo simulation were done to estimate feed-down contributions from 7 and 8 photon reaction with one and two missing photons, respectively, which remain in our final event selection. It was found that the contributions of $\omega\eta\pi^0$ (5.4 ± 0.2) %, and $\omega\pi^0\pi^0$ $(5.2 \pm 0.2)\%$, were mostly confined to the diagonal edge of the Dalitz plot, in the region of $f_2(1270)$ and $f_0(1370)$. The contributions of $4\pi^0$ was estimated as $(2.3 \pm 0.1)\%$, and was mostly confined to the region around $a_2(1320)$. The overall efficiency of our $\eta\eta\pi^0$ selection was estimated by MC simulation to be $(4.26 \pm 0.1)\%$. Taking account of the feed-down contributions in the total yield, we obtain the total cross section corresponding to the $\eta\eta\pi^0$ events in the Dalitz plot, $\sigma(\eta\eta\pi^0) = 150 \pm 1(stat) \pm 2(syst)$ nb.

III. FORMALISM FOR DALITZ-PLOT ANALYSIS

The reaction $\bar{p}p \rightarrow \eta\eta\pi^0$ is described in the isobar model as a two step process, $\bar{p}p \rightarrow f_J + \pi^0$, or $a_J + \eta$, followed by $f_J \rightarrow \eta\eta$, and $a_J \rightarrow \eta\pi^0$. In principle both the production and the decay of f_J and a_J should be independently taken into account. In practice, this is not possible. At an incident antiproton momentum of 5.2 GeV/c, $p\bar{p}$ annihilation involves angular momentum up to ~ 7 in the initial state. This makes it essentially impossible to use the full helicity formalism for the analysis of our data. Instead, we use the decay formalism developed and successfully used in several Dalitz plot analyses of the Crystal Barrel $p\bar{p}$ annihilation data at 1.94 GeV/c [5, 6, 7]. In addition, we take account of the production amplitudes in an average way by parameterizing them as a function of even powers of $\cos\theta$, where θ is the resonance production angle with respect to the $\bar{p}$ direction, $p(\theta) = 1 + \sum_{i=1}^{n} p_i \cos^{2i}\theta$. The final amplitude for the formation and decay of a resonance with spin J, projection $\lambda \equiv J_x$, mass m_0 and width Γ_0 is the given by

$$A_J^\lambda = p(\theta)G_\lambda e^{i\delta_\lambda} F_J(q) \frac{Y_J^\lambda(\alpha,\beta)}{m_0^2 - s - im_0\Gamma_m}, \quad (1)$$

where G_λ and the δ_λ are the magnitude and the phase of the complex coupling constant, $Y_J^\lambda(\alpha,\beta)$ are spherical harmonics which are functions of angles α and β, the polar and azimuthal angles of the decay in the rest frame of the resonance. The denominator is that for the relativistic Breit Wigner with energy dependent width,

$$\Gamma_m = \Gamma_0 \left(\frac{qF_J^2(q)}{m} \right) / \left(\frac{q_0 F_J^2(q_0)}{m_0} \right) \quad m = \sqrt{s}. \quad (2)$$

Here $F_J(q)$ are the Blatt-Weisskopf barrier factors for the resonance break-up momentum q (subscripts 0 denote values at the resonance mass, m_0), evaluated for a radius of 1 fermi. The combined intensities of two interfering resonances 1, and 2 in the Dalitz plot are given by

$$w_{1,2} = \sum_\lambda [|A_{\lambda,1}|^2 + |A_{\lambda,2}|^2 + 2c_\lambda\Re(A_{\lambda,1}A_{\lambda,2}^*)], \quad (3)$$

where the interference coefficient c_λ ranges from 0 (no coherence) to ± 1 (maximum coherence). We wish to note here that when two resonances interfere the difference between their phase angles, $\Delta(\delta_A)$ also becomes important. In considering interferences a certain pragmatic compromise has to be made. With 11 different resonances in our final result (see Table II), if all possible two state interferences, including self-interference were taken into account, one would need $(60 \times \lambda$ multiple) values of c_λ. This is impossible and also unnecessary. In the present work a large number of possible interferences were studied, but only those were retained in the final analysis which improved the log-likelihood by more than 20 per additional degree of freedom. The negative log-likelihood of a MC fit to the data was defined as

$$-lnL = Nln(\sum_{i=1}^{M} w_i^{MC}) - (\sum_{i=1}^{N} lnw_i^{DATA}), \quad (4)$$

where w_i^{DATA} refer to the N events in the data, and w_i^{MC} refer to the M events in the MC fit.

With this definition an increase of $\Delta(lnL) = (0.5 \times r)$ with increase of r degrees of freedom corresponds to a one standard deviation $(\Delta\chi^2/d.o.f. = 1)$ improvement in the fit. For making the final fits m_0, Γ_0 and J are manually varied, $p(\theta)$ are separately fit, and the free parameters for the fit are G_λ, δ_λ and c_λ. As detailed below, in practice much more demanding criteria for $\Delta(\ln L)$ were used.

The ingredients of fitting the Dalitz plot are masses, widths, J^{PC}, the production amplitude parameters $p(\theta)$, and resonance-resonance interferences including self-interference. We take these into account successively. We start with a basic set of six resonances. These include those which are identifiable as clear enhancements in the Dalitz plot, $f_0(1500)$, $f_0(1710)$, and $f_2(2150)$ as representative of the broad enhancements in the $M(\eta\eta) \sim 2000 - 2200$ MeV region, and $a_2(1320)$. In this basic set we also include $a_2(1700)$ and $a_4(2040)$ which are not apparent as identifiable enhancements, but which are considered well established and whose decay in $\eta\pi^0$ has been observed [3].

The initial fit with this set of resonances was done at the simplest level. Their masses and widths were fixed at PDG values [3], neither the the angular distribution of the production amplitudes, nor resonance-resonance interference was included, and only the ten G_λ were fitted by maximizing $-lnL$. The fit was quite poor, with $lnL/\#par. = -9,520/10$.

As a first step in improving the fit, it was decided to take account of the fact that at 5.2 GeV/c the production amplitudes are far from isotropic. It was found that their angular distributions could be satisfactorily parameterized as a third order polynomial in $cos^2(\theta)$. This added 18 parameters in the fit which improved by $\Delta lnL/\Delta\#par. = 5,261/18$. Inclusion of the strong self-interference of
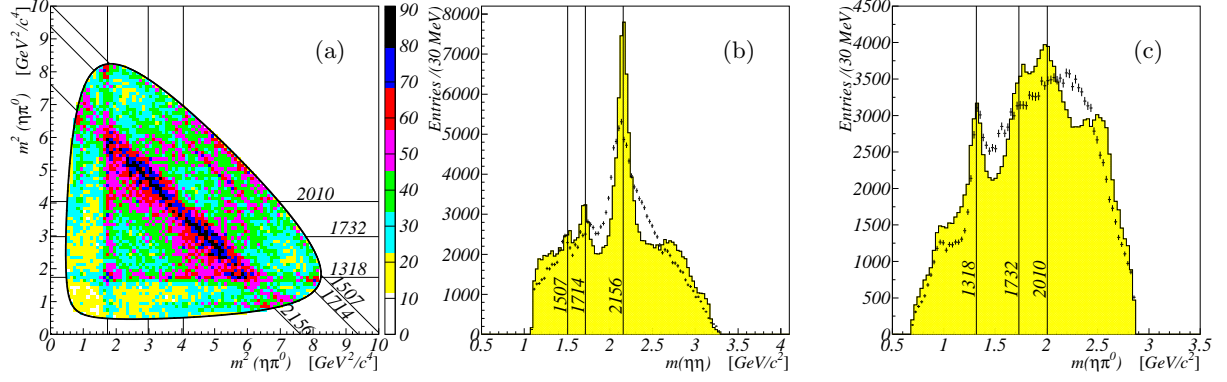
FIG. 1: (a) Dalitz plot of $\eta\eta\pi^0$. (b) and (c) show $\eta\eta$ and $\eta\pi^0$ mass projections. The positions of the resonances used in the initial fit are indicated at their PDG mass values in MeV. The histograms show the relatively poor fit obtained with this initial set of resonances, as described in the text.
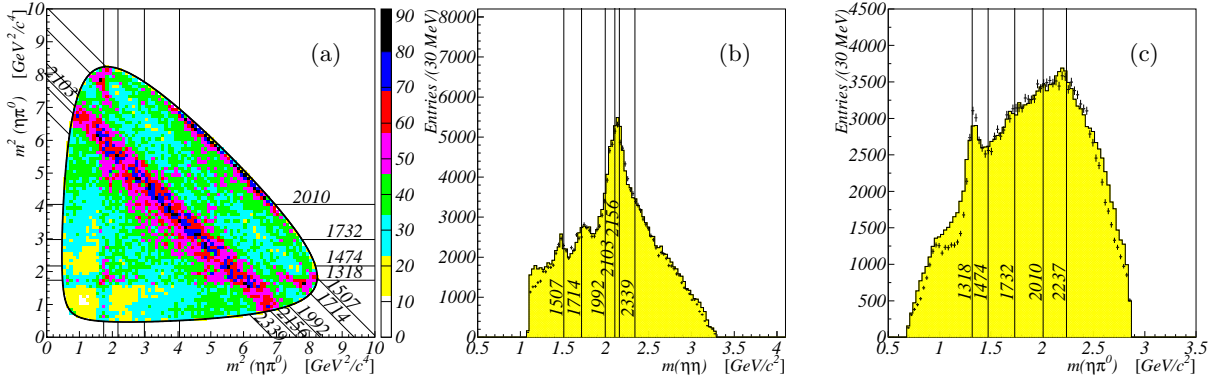

FIG. 2: (a) The best fit for the Dalitz Plot, and the corresponding invariant mass projections, (b) $\eta\eta$, and (c) $\eta\pi^0$. Data are shown with points. Histograms show the best fit using the final set of resonances.

Resonance	$\Delta lnL/\Delta\#param.$	Interference	$\Delta lnL/\Delta\#param.$	c_0	$\Delta(\delta_0)$	c_1	$\Delta(\delta_1)$
$f_0(2020)$	1464/1	$a_4(2040) \times a_4(2040)$	363/2	-0.51	0	-1.00	0
$f_0(2100)$	158/1	$a_4(2040) \times a_2(1320)$	168/4	0.83	0.06	1.00	0.41
$f_2(2340)$	878/2	$a_4(2040) \times f_2(2150)$	155/4	-0.48	1.29	-1.00	1.36
$a_0(1450)$	297/1	$a_4(2240) \times a_4(2240)$	254/2	-0.80	0	-0.83	0
$a_4(2240)$	267/2	$a_2(1320) \times f_0(2100)$	161/2	-1.00	0.17	-	-

TABLE I: Resonances and interferences added in the second iteration. c_λ and $\Delta(\delta_\lambda)$ ($\lambda = 0, 1$) refer to the interference coefficients and the phase differences (in radians) between the interfering resonances.

$a_4(2040)$ led to an additional $\Delta lnL/\Delta\#par. = 363/2$, bringing the net $-lnL/\#par. = 15,144/30$. The resulting fit is shown in Fig. 1-(b) and (c), for the projections of invariant masses $M(\eta\eta)$ and $M(\eta\pi^0)$, respectively. Both are rather poorly fit, and it is obvious that additional resonances and interferences must be considered.

The additional resonances input include $f_0(2020)$, $f_0(2100)$, $f_2(2340)$, and $a_0(1450)$, which are not considered by PDG as firmly established, and a new state $a_4(2240)$. As shown in Table I, the log-likelihood im-

provements due to the inclusion of these resonances is in all cases more than 130 per added parameter. Further, only those interferences are included which increase log-likelihood by more than ~ 40 per added parameter. Fig. 2 shows the much improved fit to the mass projections.

For the finally chosen resonances two dimensional optimization of the mass and width was done for different J^{PC} assignments. The final result of the optimization was $-lnL/\#par. = 19894/44$.
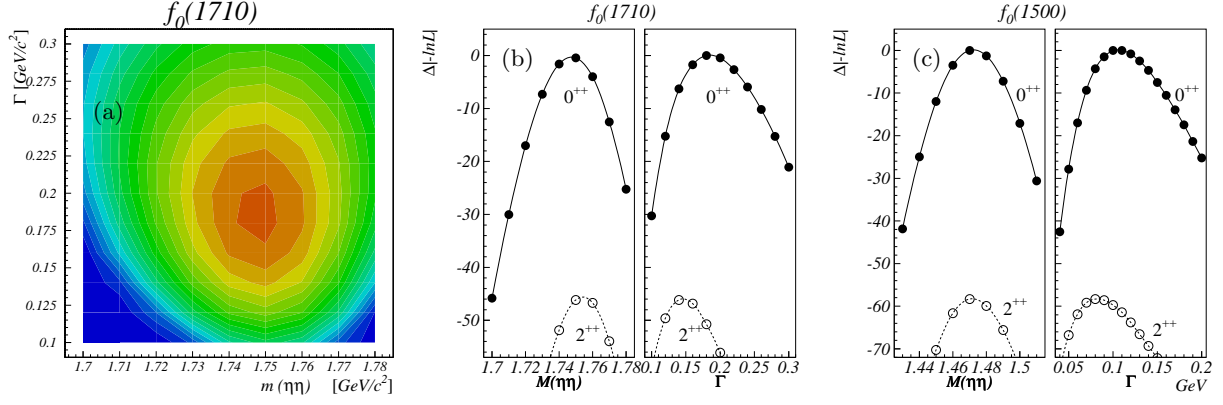
FIG. 3: Results for $\Delta|-lnL|$ optimization of mass and width: (a) contour plot for $f_0(1710)$, (b) $\Delta|-lnL|$ variation for mass and width for $f_J(1710)$, $J^{PC} = 0^{++}$ and 2^{++}, (c) same for $f_J(1500)$
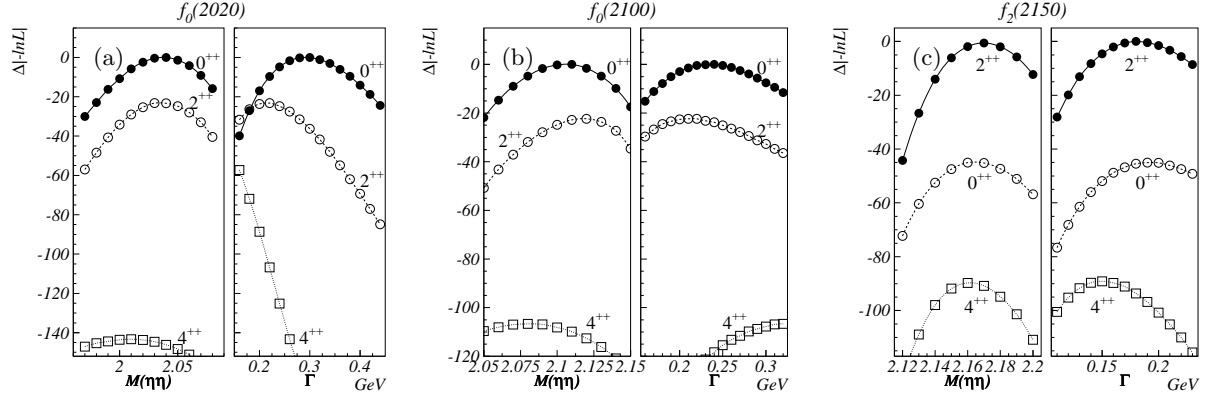

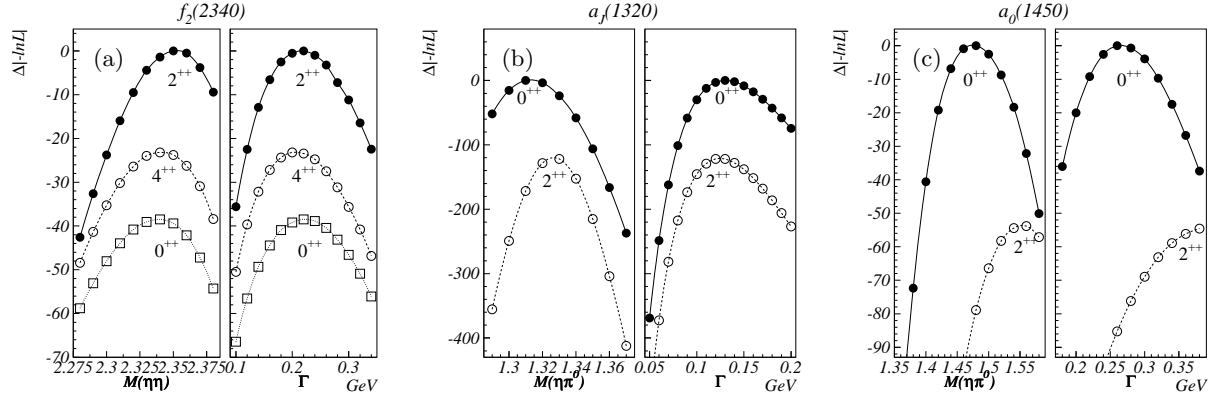FIG. 4: Results for $\Delta|-lnL|$ optimization for (a) $f_0(2020)$, (b) $f_0(2100)$, and $f_2(2150)$.

FIG. 5: Results for $\Delta|-lnL|$ optimization for (a) $f_2(2340)$, (b) $a_J(1320)$, and $a_0(1450)$.

IV. RESULTS AND DISCUSSION

Fig. 2 shows the overall results of the best fit to the Dalitz plot and the mass projections for $M(\eta\eta)$ and $M(\eta\pi^0)$. Our final results are summarized in Table II, along with the corresponding results from PDG [3]. We wish to note that the relative intensity fractions listed in Table II are related to, but not the same as relative branching fractions. This is partly due to the approximations inherent in the formalism used in our partial wave analysis, and partly because the anticuts we have imposed in event selection have different effects in different parts of the Dalitz plot. Also, interferences have been omitted in evaluating these fractions, which therefore do not add to 100%. The last column in the table lists the change in log-likelihood if a particular resonance
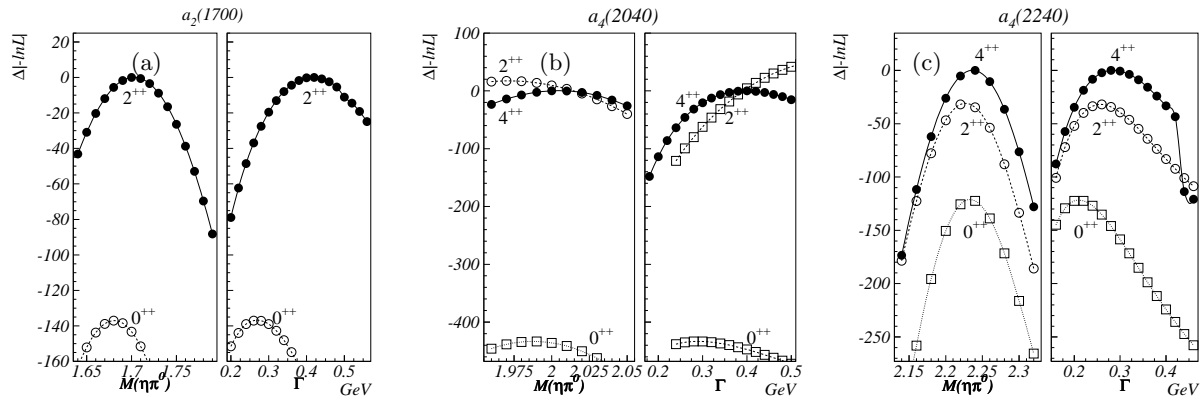
FIG. 6: Results for $\Delta|-lnL|$ optimization for (a) $a_2(1700)$, (b) $a_4(2040)$, and (c) $a_4(2240)$.

is dropped from the fit, and the parameters of all other resonances are reoptimized. This provides information about the relative importance of a resonance which is complementary to that given by its relative intensity. We now briefly discuss results shown in Figs. $3-6$ for individual resonances.

Our procedure for obtaining the best fit values of the parameters of a resonance is illustrated in Fig. 3(a,b) with the results for $f_J(1710)$. The $|-lnL|$ is calculated for specific values of mass, width, and J^{PC} of $f_0(1710)$. The results are fitted with smooth curves to determine the best fit values of M and Γ corresponding to the maxima in $|-lnL|$. Fig. 3(b) shows that the $J^{PC} = 0^{++}$ solution is clearly preferred. The corresponding contour plot for M/Γ is shown in Fig. 3(a). The same procedure was followed for $f_J(1500)$, whose results are shown in Fig. 3(c). Again $J^{PC} = 0^{++}$ is clearly preferred by $\Delta(-\ln L) = 46$. The results for other resonances are shown are shown in Figs. 4, 5, and 6. In all but one case the $|-lnL|$ differences between the different spin choices are large, and the spin assignment with the largest $|-lnL|$ (shown with solid points) is preferred; the others, (shown with open points) are rejected. For $a_J(2040)$ (Fig. 6), although the $|-lnL|$ values for $J^{PC} = 2^{++}$ and 4^{++} are comparable, no maxima are found for either M or Γ for $J^{PC} = 2^{++}$, and it is also rejected.

A. The Isoscalar States f_0 and f_2.

As already mentioned, Fig. 3 clearly shows that both $f_0(1500)$ and $f_0(1710)$ have $J^{PC} = 0^{++}$. The $J^{PC} = 0^{++}$ assignment is preferred over 2^{++} by $\Delta lnL = 58$ for $f_0(1500)$, and $\Delta lnL = 46$ for $f_0(1710)$. As listed in Table II, for $f_0(1500)$ our mass is ~ 30 MeV smaller than the PDG average, but the width is identical. For $f_0(1710)$ our mass is ~ 30 MeV larger, and the width is also $\sim 30\%$ larger. We note that the Crystal Barrel has reported that while they do observe $f_0(1500)$, they do not find any evidence for $f_0(1710)$ excitation in the $\bar{p}p \to \eta\eta\pi^0$ reaction in $\bar{p}p$ annihilation at either 0.9 GeV/c [8] or 1.94 GeV/c

[5]. On the other hand, WA102 [9] reports excitation of both $f_0(1500)$ and $f_0(1710)$ in central production with decay into $\eta\eta$. We find that in our $\bar{p}p \to \eta\eta\pi^0$ measurement at 5.2 GeV/c, in the Dalitz plot the ratio of the intensities $(f_0(1710) \to \eta\eta)/(f_0(1500) \to \eta\eta) \sim 2.2$. We note that Amsler et al. [8] report this ratio to be < 0.25 (90% CL) for production in $p\bar{p}$ annihilation at 0.9 GeV/c. Hopefully, our result provides a new input in the continuing discussion about the scalar glueball admixtures in these two states.

Although the observation of the isoscalars $f_0(2020)$ and $f_0(2100)$ has been reported before, PDG'04 considers them unconfirmed. We find $f_0(2020)$ and $f_0(2100)$ with masses and widths listed in the Table II to be strongly populated with nearly equal intensity. Once again the 0^{++} assignments are preferred for both over 2^{++} assignments by $\Delta lnL = 23$ and 22, respectively. In a global analysis of the Crystal Barrel data for momenta 900-1900 MeV/c Anisovich et al. [10] identify these two scalars decaying into $\eta\eta$ as having mass/width of $(2005\pm30)/(305\pm50)$ MeV and $(2105\pm15)/(200\pm25)$ MeV, which are in almost exact agreement with ours. We also note that a combined enhancement of these two states was reported as X(2100) decaying into $\eta\eta$ by the earlier Fermilab E760 experiment [11]. Its J^{PC} was not determined.

Although ten f_2-states have been reported in our mass region by different experiments, the PDG regards only four, $f_2'(1525)$, $f_2(2010)$, $f_2(2300)$ and $f_2(2340)$ as sufficiently well established to be included in the meson summary list. None of these except $f_2'(1525)$ have been observed to decay into $\eta\eta$. We find no evidence for the excitation of $f_2'(1525)$, although it is possible that its resolution is rendered impossible due to the presence of nearby stronger $f_0(1500)$. The lnL plot in Fig. 3(c) suggests that $f_2(1525)$ population is very small, if not zero. Similarly, we find no evidence for $f_2(2010)$. We confirm the existence of $f_2(2150)$ which has been omitted by PDG from its summary list, but which was previously observed to decay into $\eta\eta$ by WA102 [9]. Our mass and width are in good agreement with both WA102 and the PDG ave-

Resonance	Mass(MeV)		J^{PC}	Width(MeV)		Rel. Int.	If removed
	PDG'04	Present		PDG'04	Present	%	$\frac{\Delta lnL}{\Delta \#par.}$
$f_0(1500)$	1507 ± 5	1473 ± 5	0^{++}	109 ± 7	108 ± 9	2.4	207/1
$f_0(1710)$	1714 ± 5	1747 ± 5	0^{++}	140 ± 10	188 ± 13	5.2	521/3
$f_0(2020)^{*\dagger}$	1992 ± 16	2037 ± 8	0^{++}	442 ± 60	296 ± 17	10.9	295/3
$f_0(2100)^{*\dagger}$	2103 ± 7	2105 ± 8	0^{++}	206 ± 15	236 ± 14	7.9	249/3
$f_2(2150)^*$	2156 ± 11	2170 ± 6	2^{++}	167 ± 30	182 ± 11	6.5	209/6
$f_2(2340)^{*\dagger}$	2339 ± 55	2350 ± 7	2^{++}	319^{+81}_{-69}	218 ± 16	4.8	124/2
$a_2(1320)$	1318 ± 1	1327 ± 2	2^{++}	111 ± 2	128 ± 4	6.5	2335/14
$a_0(1450)$	1474 ± 19	1477 ± 10	0^{++}	265 ± 13	267 ± 11	3.9	418/5
$a_2(1700)^*$	1732 ± 16	1702 ± 7	2^{++}	194 ± 40	417 ± 19	20.6	1185/4
$a_4(2040)$	2010 ± 12	2004 ± 6	4^{++}	353 ± 40	401 ± 16	20.1	738/13
$a_4(2237)^*$	–	2237 ± 5	4^{++}	–	291 ± 12	20.7	823/4

TABLE II: Results for masses, widths and J^{PC} of light quark resonances decaying into $\eta\eta$ and $\eta\pi^0$ as seen in $\bar{p}p \to \pi^0\eta\eta$ at 5.2 GeV/c. All errors are statistical only and correspond to $\Delta|-lnL| = 0.5$ or $\Delta\chi^2 = \pm 1\sigma$. Asterisks* mark states presently omitted from meson summary list of PDG'04. Daggers† mark f-states which have not been seen in $\eta\eta$ before. For explanation of the last two columns, see text.

rage. We also observe clear evidence for $f_2(2340)$. Etkin *et al.* [12] had claimed this as a doublet, $f_2(2300)$ and $f_2(2340)$, in its $\phi\phi$ decay. We do not find any evidence for such a close mass doublet.

We note that we do not find any evidence for the tensor glueball candidate $\xi(2230)$, or $f_2(2230)$ decaying into $\eta\eta$. This is consistent with the result of the Crystal Barrel search for the same [13].

B. The Isovector States a_0, a_2 and a_4.

Our fit to the $\eta\pi^0$ mass spectrum (see fig. 2(c)) is admittedly poorer compared to the isoscalar state in fig 2(b). It also presents a certain vexing problem concerning the strong enhancement observed at mass ~ 1320 MeV, which is followed by a dip in the vicinity of 1450 MeV. The $a_2(1320)$ is a well established tensor resonance with PDG mass/width, $M/\Gamma = (1318.3 \pm 0.6)/(105 - 111)$ MeV. It is strongly populated in many reactions, and its decays into several channels, including $\eta\pi^0$, are well documented [3]. A scalar $a_0(1450)$ with $M/\Gamma = (1470 \pm 25)/(265 \pm 30)$ MeV decaying into $\eta\pi^0$ was reported by CB [14] in $\bar{p}p$ annihilation at rest, and also in $K_L K^\pm$ [15].

On the other hand, OBELIX [16] has reported a scalar with $M/\Gamma = (1290 \pm 10)/(80 \pm 5)$ in $\bar{p}p$ annihilation decaying into $K^\mp K_S^0$, along with a nearly factor five weaker excitation of $a_2(1320)$ than what follows from the PDG averages. We have examined the possible existence of $a_0(1290)$ of OBELIX. As shown in Fig. 5(b) and Table II we obtain a good fit to our data with $a_2(1320)$ and $a_0(1450)$, with the best fit M/Γ parameters for both, a_2: $M/\Gamma = (1327 \pm 2)/(128 \pm 4)$ MeV and a_0: $M/\Gamma = (1477 \pm 10)/(267 \pm 11)$, both in excellent agreement with the PDG'04 values. Paradoxically, an even

better fit (not shown) is obtained with $a_0(1290)$ with $M/\Gamma = (1314 \pm 2)/(133 \pm 4)$ MeV and $a_0(1450)$ with $M/\Gamma = (1404 \pm 9)/(222 \pm 18)$ MeV. With a 66% (or 8.3σ) larger width for $a_0(1290)$ than that reported by OBELIX (133 ± 4 MeV versus 80 ± 5 MeV) it is unlikely that this solution represents their resonance. However, this still poses the question whether both $a_2(1320)$ and $a_0(1290)$ can coexist. We have studied this question at length, considered additional interferences, and conclude that if both resonances exists, it is not possible to resolve them. We list the results for the $J = 2$ assignment in Table II because of the weight of numerous final states, including $\eta\pi$, in which $a_2(1320)$ has been observed, and not $a_0(1290)$. Nevertheless, we must consider the ambiguity between $a_2(1320)$ and $a_0(1290)$ as unresolved.

We confirm $a_4(2040)$ with parameters in excellent agreement with those in PDG'04. We confirm $a_2(1700)$ but find it to have much larger width than PDG'04. We find a strong resonance, $a_4(2237)$ decaying into $\eta\pi$, with $M/\Gamma = (2237 \pm 5)/(291 \pm 15)$ MeV. A $J^{PC} = 4^{++}$ resonance decaying into $\eta\pi$ and $\eta'\pi$ was earlier reported by Anisovich et al. [17].

Additional resonances which were tried in the fit were $a_0(980)$, $f_0(1370)$, $f_2'(1525)$, $f_2(1640)$, $f_2(1910)$, $\pi_1(1400)$, $\pi_1(1600)$, $f_0(1710 - 1790)$, $f_2(1870 - 1910)$. None of these obtain significant contributions ($> 0.5\%$) to the intensity. As mentioned earlier, the resonances near the boundaries of the Dalitz Plot, particularly $a_0(980)$ and $f_0(1370)$, suffer from the effect of the 'anticuts'. No convergence was obtained when the reported hybrids $\pi_1(1400)$ and $\pi_1(1600)$ were included in the fits.

[1] C. Amsler, Rev. Mod. Phys. **70**, 129 (1998); S. Godfrey and J. Napolitano, Rev. Mod. Phys. **71**, 1411 (1999).

[2] See, for example, S. Godfrey and N. Isgur, Phys. Rev. D **32**, 189 (1985).

[3] S. Eidelman *et al.* [Particle Data Group], Phys. Lett. B **592**, 1 (2004).

[4] G. Garzoglio *et al.*, Nucl. Instrum. Meth. A **519**, 558 (2004).

[5] A. Abele *et al.* (Crystal Barrel Collaboration), Eur. Phys. J. **C 8**, 67 (1999).

[6] J. Adomeit *et al.* (Crystal Barrel Collaboration), Z. Phys. C **71**, 227 (1996).

[7] A. V. Anisovich *et al.*, Phys. Lett. **449**, 145 (1999).

[8] C. Amsler *et al.* (Crystal Barrel Collaboration), Eur. Phys. J. **C 23**, 29 (2002).

[9] D. Barberis *et al.* (WA102 Collaboration), Phys. Lett. **B 479**, 59 (2000).

[10] A. V. Anisovich *et al.*, Nucl. Phys. **A 662**, 319 (2000).

[11] T. A. Armstrong *et al.* (E760 Collaboration), Phys. Lett. **B 307**, 394 (1993).

[12] A. Etkin *et al.*, Phys. Lett. **B 201**, 568 (1988).

[13] C. Amsler *et al.* (Crystal Barrel Collaboration), Phys. Lett. **B 520**, 175 (2001).

[14] C. Amsler *et al.* (Crystal Barrel Collaboration), Phys. Lett. **B 333**, 277 (1994).

[15] A. Abele, *et al.* (Crystal Barrel Collaboration), Phys. Rev. **D 57**, 3860 (1998).

[16] A. Bertin *et al.* (OBELIX Collaboration), Phys. Lett. **B 434**, 180 (1998).

[17] V. A. Anisovich *et al.* (Crystal Barrel Collaboration), Phys. Lett. **B 452**, 173 (1999).